



1                                    **Coastal gradients south of Cape Town:**  
2                                    **what insights can be gained from mesoscale reanalysis?**

3  
4                                    Mark R Jury  
5                                    Univ Zululand, South Africa and Univ Puerto Rico Mayaguez, PR, USA

6  
7  
8    **Abstract**

9    Mesoscale datasets are used to study coastal gradients in the marine climate and oceanogra-  
10    phy south of Cape Town. Building on past work, satellite and ocean / atmosphere reanalysis  
11    are used to gain new insights on the mean structure, circulation and meteorological features.  
12    HYCOM v3 hindcasts represent a coastward reduction of mixing that enhances stratification  
13    and productivity inshore. The mean summer currents are westward  $-4$  m/s along the shelf  
14    edge and weakly clockwise within False Bay. The marine climate is dominated by southeast-  
15    erly winds that accelerate over the mountains south of Cape Town and fan out producing dry  
16    weather. Virtual buoy time series in Dec 2012-Feb 2013 exhibit weather-pulsed upwelling in  
17    early summer interspersed with quiescent spells in late summer. Intercomparisons between  
18    model, satellite and station data build confidence that coupled reanalyses yield opportunities  
19    to study air-sea interactions in coastal zones with complex topography. The  $0.083^\circ$  HYCOM  
20    reanalysis has 16 data points in the embayment south of Cape Town, just adequate to resolve  
21    the coastal gradient and its impacts on ocean productivity.

22  
23  
24  
25  
26  
27

mark.jury@upr.edu



28 **Introduction**

29 The coastal zone south of Cape Town, South Africa is comprised of linear sandy beaches and  
30 a semi-enclosed bay surrounded by mountains (Fig 1a,b). False Bay is southward facing and  
31 about  $10^3$  km<sup>2</sup>, with the Cape Peninsula to the west and Cape Hangklip to the east. The shelf  
32 oceanography exhibits a range of conditions from seasonally pulsed upwelling events (Shan-  
33 non and Field 1985, Lutjeharms and Stockton 1991, Largier et al. 1992, Dufois and Rouault  
34 2012) to warm-water intrusions from the Agulhas Current, creating great biological diversity  
35 (Griffiths et al. 2010). The upper ocean circulation tends to be northwestward and pulsed at  
36 subseasonal time scales by passing weather, shelf waves, warm rings and tides (Grundlingh  
37 and Larger 1991; Nelson et al 1991). Coastal winds and temperatures exhibit sharp cross-  
38 shelf gradients (Jury 1991, VanBallegooyen 1991) depending on latitude fluctuations of the  
39 subtropical anticyclone.

40 The high pressure cells of the South Atlantic and South Indian Ocean tend to join in summer  
41 and produce dry weather and upwelling-favourable winds from the southeast that are shallow  
42 and diverted around the >1000 m mountains of Cape Hangklip and the Cape Peninsula. The  
43 winds accelerate off the capes and form shadow zones over leeward bays, creating cyclonic  
44 vorticity that enhances upwelling (Wainman et al. 1987, Grundlingh and Largier 1991,  
45 Jacobson et al. 2014). Winds entering False Bay become channeled N-S and tend to induce  
46 standing clockwise rotors in the upper ocean (deVos et al. 2014), which are pulsed by geo-  
47 strophic currents across the mouth.

48 With the passage of eastward-moving atmospheric Rossby waves across the southern tip of  
49 Africa at 3-20 day intervals (Jury and Brundrit 1992), the subtropical ridge is replaced by  
50 coastal lows followed by downwelling-favourable northwesterly winds and frontal troughs  
51 that bring rainfall, stormy seas, onshore transport and mixing – most often in winter: May-  
52 Sep. (Engelbrecht et al. 2011, Schilperoort et al. 2013, deVos et al. 2014, Rautenbach 2014).

53 The city of Cape Town, its 4 million residents (Statistics SA 2020) and associated infrastruc-  
54 ture have intensified anthropogenic pressure on the southern coastal zone. Sandy beaches  
55 there are vulnerable to sediment loss from rising seas and recreational use (Mather et al.  
56 2009, Theron et al. 2010; Roux & Toms 2013, Theron et al. 2014). Climate-change has be-  
57 come manifested in longer summers and a southeastward shift in wind-driven upwelling, ma-  
58 rine ecosystems and fisheries (Rouault et al. 2010, Lloyd et al. 2012, Blamey et al. 2012,  
59 Schlegel et al. 2017).



60 Coastal embayments tend to be very productive and False Bay is no exception. Brown et al.  
61 (1991) reported an average chlorophyll concentration of  $4 \text{ mg m}^{-3}$  in the euphotic layer, that  
62 varies from summer to winter:  $5.5$  vs  $2.1 \text{ mg m}^{-3}$  (Giljam 2002). Nutrients enter the southern  
63 coastal zone via runoff and municipal waste streams (Parsons 2000, Taljaard et al. 2000).  
64 Although numerous small rivers drain into False Bay, the nutrients supplied by upwelling  
65 exceed those from terrestrial sources (Taljaard 1991, Giljam 2002). Coastal and offshore wa-  
66 ters show healthy rates of exchange, particularly during stormy spells that induce surf-zone  
67 currents.

68 Our understanding of the physical oceanography south of Cape Town has benefited from  
69 studies of the upper ocean circulation (Botes 1988), the wind field and the variability of sea  
70 temperatures (Dufois et al. 2012). Yet many processes governing intra-seasonal variability  
71 remain obscure (Wainman et al. 1987). There is a lack of consensus on the mean seasonal  
72 circulation (Grundlingh et al. 1989, Taljaard et al. 2000), despite ample knowledge of the air-  
73 sea interactions. To overcome the limited scale and brevity of measurement campaigns, mod-  
74 elling efforts (eg. Penven et al. 2001) have elucidated coastal features over a longer period.  
75 Hydrodynamic simulations with temporal forcing by Nicholson (2011) gave promising re-  
76 sults, and Coleman (2019) recently modelled the circulation south of Cape Town forced with  
77 daily data from the Hybrid-Coordinate Ocean Model (HYCOM; Cummings and Smedstad  
78 2013) and the Weather Research and Forecasting model (WRF; Skamarock et al. 2008).  
79 Coleman (2019) found sheared clockwise circulations during summer, and favourable valida-  
80 tions for mean currents and thermal stratification in False Bay.

81 Given the above history of scientific endeavors, the objective of this work is to embark on a  
82 new mission to utilize the global ocean data assimilation system to describe the spatial pattern  
83 and temporal variability of the marine environment. We demonstrate that mesoscale reanaly-  
84 sis offers valuable new insights on the coastal gradient in summer climate and physical  
85 oceanography south of Cape Town.

## 86 **Data**

87 Marine climate variability is described using weather and wave reanalysis products at 20-30  
88 km resolution, namely CFSr2, ECMWF, Wavewatch3 (Saha et al. 2014, Dee et al. 2011,  
89 Tolman 2002; respectively). Coastal gradients are described using 4 km resolution satellite  
90 visible and infrared products (Reynolds et al 2002), and IMT station observations in western  
91 False Bay. Table 1 lists acronyms and dataset attributes.



92 The mesoscale oceanography south of Cape Town is studied with HYCOM v3.1 reanalysis  
93 (Cummings and Smedstad 2013; Metzger et al. 2014), that assimilates microwave, infrared  
94 and visible measurements from multiple satellites, calibrated with in-situ observations. Cli-  
95 matology, persistence and model-calculated fields are used to quality-control and nudge the  
96 incoming data, within static  $0.033^\circ$  resolution GIS fields that include bathymetry, surface  
97 roughness, etc. Running in parallel with the ocean model are operational atmosphere and land  
98 models that deliver coupled information on momentum, heat and water fluxes and feedbacks  
99 (Table 1). In the 41-layer  $0.083^\circ$  HYCOM v3.1 hindcast employed here, Navgem v1.4 3-  
100 hourly  $0.176^\circ$  resolution atmospheric data provide background initialization for kinematic  
101 and thermodynamic fields derived from satellite and insitu measurements, continually assimi-  
102 lated over a rolling 5-day window (Hurlburt et al. 2009). A hydrological sub-model assimi-  
103 lates satellite rainfall / soil moisture and predicts runoff, which is blended with satellite salini-  
104 ty measurements (Table 1). Validations have been done for the HYCOM reanalysis, and er-  
105 rors for many variables are  $< 10\%$  (Chassignet et al. 2009, Metzger et al. 2017). Hindcasts  
106 differ from operational forecast simulations in that the rate of change and evolution of spatial  
107 structure is known; the rolling 5-day analysis window has overlapping temporal information  
108 to ensure a close fit to environmental conditions. This is crucial for infrequent zenith altime-  
109 ter data which prescribes the currents. Another key point is that post-2008 reanalysis better  
110 characterizes the nearshore oceanography due to finer microwave footprints that reach the  
111 coast.

112 HYCOM reanalysis fields of near-surface sea temperature, salinity, currents and mixed layer  
113 depth (MLD) are analyzed as mean maps and sections. We focus on the summer of December  
114 2012 to February 2013, which coincides with VIIRS reflectance, Jason-1 -2 altimeter, and  
115 Ascatt-A -B scatterometer coverage that better constrains the physical oceanography. Cross-  
116 correlations between the various surface ocean and atmosphere parameters are studied in this  
117 90 day period. Other motivations for our study period include summer's marine productivity  
118 (Pfaff et al. 2019), and the variety of conditions attributable to pulsed upwelling and shelf  
119 wave events.

120 Insitu measurements over the coast and shelf south of Cape Town are made by numerous  
121 government agencies: South African (SA) Weather Service, Dept Environmental Affairs,  
122 Inst Marine Technology (IMT), Centre for Scientific and Industrial Research Marine Dept,  
123 SA Dept Water Affairs, SA Hydrographic Dept; with data operationally reported and subse-  
124 quently archived at the SA Data Centre for Oceanography. The Univ Cape Town Oceanogra-



125 phy Dept hosts short-term projects and regional ocean numerical modelling.  
126 Evaluating the ‘influence’ of surface reports in operational data assimilation (Table 2), values  
127 of ~24% in False Bay contrast with ~90% inland. This trend continues for upper ocean T/S  
128 observations that are nearly four times greater in Table Bay than False Bay (WOA 2013).  
129 Hence our analysis of marine conditions over the shelf south of Cape Town relies more on  
130 satellite and model than in-situ observations.

131 Comparisons of HYCOM reanalysis ocean data with daily gauge and radiometer measure-  
132 ments show reasonable agreement (cf. Appendix A-1a,b) in the period 2008-2015. The sea  
133 surface height comparison has a 24% fit with discrepancies attributable to coastal tide residu-  
134 als and non co-location. Sea temperatures have a 38% fit and diverge in warm spells, the  
135 model tending to over-estimate. Comparison of ECMWF-5 reanalysis and Simonstown sta-  
136 tion hourly weather data in the period Dec 12 - Feb 13 (cf. Appendix-1c,d) are good for pres-  
137 sure (88%) and wind speed (62%) but lower for air temperature (21%) presumably because  
138 the 0.3° reanalysis has contributions from land. Coleman (2019) reports similar validations  
139 for the summer of 2010.

140 The HYCOM reanalysis has limited atmospheric outputs, so to evaluate the wind circulation  
141 south of Cape Town, the WRFv3.8 model (Skamarock et al. 2008) is used to downscale  
142 ECMWF fields, as in the simulations of Coleman (2019). The WRF model resolution of 0.1°  
143 complies with the HYCOM reanalysis, and uses default schemes for boundary layer, flux  
144 transport, radiative transfer and surface coupling. We focus on the nature of horizontal flow  
145 over False Bay during summer Dec 12 - Feb 13, a period of ‘near normal’ climate, eg. sea  
146 level air pressure anomaly ~ 0 hPa.

## 147 **Results**

### 148 **Summer climate and weather**

149 We first consider the coast and climate before analyzing the shelf and ocean. Warm dry  
150 weather and sparse vegetation characterize summer (Fig 2a,b). Satellite land surface tempera-  
151 tures exhibit sharp gradients from the Cape Flats (40C at 34S) to cool southern coasts (25C at  
152 34.4S), similar to Tadross et al. (2012). Little rainfall occurs in summer so terrestrial vegeta-  
153 tion is depleted and ocean salinity is controlled by evaporation and currents, not terrestrial  
154 run-off.

155 Figure 2c,d illustrates the spatial pattern of ECMWF WRF-downscaled surface winds over  
156 the False Bay region in morning and afternoon. The mean southeasterly winds pass Cape



157 Hangklip and reach 9 m/s in mid-bay. The flow acceleration is attributed to: 1. orographic  
158 channeling (Venturi), 2. vertical constraint by trade wind inversion, and 3. sinking motion  
159 from declining coriolis and sensible heat flux (cf. Jury and Reason 1989). Summer winds are  
160 characterized by a low-level wind jet over False Bay, seen in earlier aircraft surveys (Jury  
161 1991), which is embedded in a shallow moist layer (cf. Appendix A-2a). Diurnal variability is  
162 of high amplitude as evident below.

163 Time series of CFSr2 winds over the coast and shelf (Fig 2e,f) show a meridional component  
164 that is positive and steady except for brief reversals at the end of December 2012 and Febru-  
165 ary 2013. The zonal wind component is negative and fluctuating particularly in mid-January  
166 2013. The coastal gradient is small for mean meridional flow: shelf  $V = 3$  m/s vs coast 1.6  
167 m/s, however the standard deviation of zonal winds is shelf  $U = 6.6$  m/s vs coast 2 m/s. Dur-  
168 ing spells of strong easterlies from transient anticyclones, the wind vorticity contribution to  
169 coastal upwelling is dominated by the gradient of  $\partial U/\partial y$ .

170 Time series of 6-hourly CFSr2 thermal variables (Fig 2 g,h) show large air-sea differences, as  
171 expected. Coastal air temperatures fluctuate diurnally from 15-35C while shelf temperatures  
172 rise gradually from 18 to 21C over the summer. Standard deviations vary from shelf 0.4C to  
173 coast 5.7C. The landward increase of temperature drives a seabreeze contribution to the mean  
174 meridional flow. The CFSr2 surface heat fluxes show diurnal amplitude 0-300 W/m<sup>2</sup> over the  
175 coast, but stay in the range 50-100 W/m<sup>2</sup> at the shelf edge. Hence the 0.2° CFSr2 captures the  
176 coastal gradients that govern the shelf oceanography, with attributes consistent with Navgem  
177 v1.4 that underpins the HYCOM reanalysis.

178 Considering the air pressure record from the weather station in western False Bay and match-  
179 ing ECMWF v5 reanalysis (cf. Appendix A-1d), we note sharp dips < 1005 hPa on 27 Dec,  
180 29 Jan, 9 Feb, and 17 Feb. These identify coastal low passage associated with trapped shelf  
181 waves. In the 27 Dec and 17 Feb cases, the (station) wind reversed from 15 m/s SE (before)  
182 to 12 m/s NW (after). CFSr2 wind vorticity and sub-surface vertical motions in False Bay (pt  
183 3) changed from  $-5 \cdot 10^{-4} \text{ s}^{-1} / +0.7 \text{ m/day}$  (before) to  $+4 \cdot 10^{-4} \text{ s}^{-1} / -0.8 \text{ m/day}$  (after) and (buoy)  
184 sea temperatures dropped below 15C the following day. These abrupt changes in environ-  
185 mental forcing are buffered by the semi-enclosed nature of False Bay, thus sustaining produc-  
186 tivity.

### 187 **Shelf Oceanography**

188 In this section we characterize the shelf oceanography south of Cape Town. The shelf edge



189 has cooler waters and lower salinity due to upwelling (Fig 3a). Equatorward winds drive sur-  
190 face currents into False Bay, trapping a warm salty zone against the north coast  $>35.3$  g/kg  
191 (Fig 3a), consistent with Dufois and Rouault (2012). The summer water flux is negative  
192 across the region during summer (Fig 3b), as evaporation of 4-6 mm/day exceeds precipita-  
193 tion of 1-2 mm/day. Fast and divergent winds dessicate the Cape Peninsula in contrast with  
194 orographic lifting over the eastern mountains. Hence the P – E field varies from neutral inside  
195 False Bay to strongly negative west of Cape Town.

196 False Bay has a narrow exposure to the Southern Ocean. SW swells of  $\sim 3$  m tend to refract  
197 into the bay producing greater energy on the east side (Fig 3c). The ocean mixed layer depth  
198 ranges from  $< 10$  m inside False Bay to  $> 50$  m outside, due to kinematic exposure and ther-  
199 mal stratification. Mean currents (Fig 3d) are weak in the northern half of False Bay, but  
200 westward at the shelf edge and drawn into the Benguela Current.

201 Winds and currents are sheared into clockwise gyres that increase water residence time ena-  
202 bling nutrient build-up and phytoplankton blooms within False Bay (chlorophyll  $> 10$  mg/m<sup>3</sup>,  
203 Fig 3e). Month-to-month changes in productivity relate to wind angle, intensity of pulsed  
204 upwelling (cf. Appendix A-2b) and prevalence of rotary circulations.

205 Figure 3f presents the Dec 12 - Feb 13 sequence of monthly SST fields based on MODIS IR  
206 satellite. There is a cold upwelling plume west of Cape Town and warm waters off the shelf  
207 in Jan-Feb 13. Yet within False Bay we find subtle structures: remnants of repeated  
208 upwelling off Cape Hangklip create a cold area in the middle of the bay, while warmer waters  
209 hug the northeastern coast, beneath the wind shadow from the eastern mountains. Sustained  
210 upwelling and widespread cold SSTs in December 2012 are replaced by warm intrusions and  
211 nearshore quiescent zones by February 2013.

212 The Dec 12 - Feb 13 mean HYCOM depth sections on 18.6E in Figure 4a-d illustrate an up-  
213 per 20 m layer with temperatures and salinity of 20C, 35.4 g/kg. Shelf-edge upwelling creates  
214 a wedge of 12C, 34.7 g/kg waters below 60 m. Zonal currents are weak inshore and strongly  
215 westward at shelf-edge above 20 m. HYCOM meridional currents reveal an overturning cir-  
216 culation, with deeper offshore flow and very shallow onshore flow. HYCOM daily time se-  
217 ries at three points along 18.6E exhibit pulsing and cooler fresher conditions in the south  
218 compared with the north (Fig 4e-g). There is a strong gradient in zonal currents from  $\sim 0.5$  m/s  
219 at shelf-edge to zero at the coast.

220 Statistical analysis is given in Table 3 and reveals that inshore (pt 1 at 34.1S) sea tempera-



221 tures are more sensitive to waves than winds, and that offshore (pt 3 at 34.3S) sea tempera-  
222 tures follow zonal winds more than currents. We note that offshore and inshore temperatures  
223 are uncorrelated, and offshore salinity is negatively related to inshore temperature. Coastal  
224 and shelf-edge salinity are correlated, and inshore salinity responds to zonal currents (-r).  
225 HYCOM zonal currents inshore and offshore associate similarly to winds at 1-day lead, and  
226 being correlated with each other – suggest that Ekman transport frequently overrides the  
227 clockwise gyre.

228 Time series of Wavewatch3 swell characteristics at coast and shelf-edge virtual buoys are  
229 given in Fig 4h-j. Swell heights offshore (pt 4 at 34.4S) oscillate around 2 m except for a  
230 spell of stormy seas at the end of December 2012. Near-shore swell heights (pt 1 at 34.1S)  
231 remain near 1 m after attenuation. Southwest swell directions prevail offshore with an occa-  
232 sional swing to southeast. Inshore directions refract to southerly and show little change. Swell  
233 periods from 9 to 13 s tend to ‘bunch’ inshore < 8 s. The 25 km W3 reanalysis captures the  
234 coastal gradient in swell properties, but finer resolution or downscaling would be ideal.

### 235 **Conclusions**

236 Mesoscale datasets were employed to study the marine climate and physical oceanography  
237 south of Cape Town during summer 2012-13. The 0.083° HYCOM v3.1 reanalysis offers  
238 new insights on the spatial and temporal nature of air-sea interactions, and consistently repre-  
239 sents a coastward reduction of mixing that enhances thermal stratification (cf. Fig 3c, 4a,b).  
240 Cross-coast gradients are particularly strong for zonal wind and current, temperature and sa-  
241 linity, and wave height. The reanalysis circulation obtains westward flow across the mouth (–  
242 0.4 m/s) and a weak clockwise gyre in mid-bay (cf. Fig 3d) that improves productivity (Fig  
243 3e). The mesoscale features seen here are consistent with Coleman (2019), whose high reso-  
244 lution model assimilated the very same HYCOM and ECMWF-WRF data. Under summer-  
245 time southeasterly winds, the clockwise gyre in False Bay was modelled to have inflow / out-  
246 flow of ~0.2 m/s on the upper-west / lower-east side, and a sea temperature increase of ~5C  
247 from deep-offshore to surface-inshore. These features ( $\partial V/\partial z$ ,  $\partial T/\partial y$ ) are reflected in the  
248 HYCOM reanalysis (cf. Fig 4d,e) and in Coleman (2019, Fig 6-22,6-26 therein).

249 Temporal variability during summer is dominated by SE winds that accelerate near Cape  
250 Hangklip and fan out across False Bay, promoting dry weather. Virtual buoy time series in  
251 Dec 12 - Feb 13 exhibit weather-pulsed upwelling, and station intercomparisons build confi-  
252 dence that coupled reanalyses yield opportunities to study air-sea interactions in coastal zones





253 with complex topography. Yet our 0.083° reanalysis has 16 data points in the embayment  
254 south of Cape Town. Finer downscaling could propagate ambiguities from microwave radi-  
255 ometers. Thus we propose that current technology allows many questions to be answered,  
256 from coastal processes to climate change. Longer summers in Cape Town could see a shift in  
257 resources from land to sea. This sentinel for global impacts on sustainable development needs  
258 on-going scientific assessment in support of holistic management.

### 259 **Acknowledgements**

260 We thank the SA Institute for Maritime Technology for provision of hourly weather station,  
261 tide gauge, and buoy data off Simonstown. 1<sup>st</sup> author recognizes on-going support from the  
262 SA Dept of Education. Sen Chiao of San José State Univ, CA provided the WRF downscaled  
263 wind fields.

### 264 **References**

- 265 Blamey, L.K., Howard, J.A.E., Agenbag, J., Jarre, A. 2012. Regime-shifts in the southern  
266 Benguela shelf and inshore region. *Prog Oceanogr.* 106, 80-95.
- 267 Botes, W. 1988. Shallow water current meters comparative study: False Bay. CSIR Report  
268 T/SEA 8803, 14; Stellenbosch.
- 269 Brown, A.C., Davies, B.R., Day, J.A., Gardiner, A.J.C. 1991. Chemical pollution loading of  
270 False Bay, in Jackson WPU ed. False Bay 21 years on - an environmental assessment. Proc.  
271 Symposium. *Trans. R. Soc. S. Afr.* 47, 703-716.
- 272 Brundrit, G. 2009. Global Climate Change and Adaptation: City of Cape Town sea-level rise  
273 risk assessment, Phase 5 Full investigation of alongshore features. City of Cape Town.
- 274 Chassignet, E.P. and co-authors. 2009. US GODAE: Global ocean prediction with the Hybrid  
275 coordinate ocean model (HYCOM). *Oceanography* 22, 64-75.
- 276 Coleman, F. 2019. The development and validation of a hydrodynamic model of False Bay,  
277 MSc thesis, Univ. Stellenbosch, 166 pp.
- 278 Cummings, J.A. and Smedstad, O.M. 2013. Variational data assimilation for the global  
279 ocean. *Data Assimilation for Atmospheric, Oceanic and Hydrologic Applications vol 2*, SK  
280 Park and L Xu eds., Springer-Verlag, 303-343.
- 281 Dee, D.P. and co-authors 2011. The ERA-interim reanalysis: configuration and performance  
282 of the data assimilation system. *Quart J Royal Meteor. Soc.* 137, 553-597.



- 283 de Vos, M., Rautenbach, C. and Ansorge, I. 2014. The inshore circulation at Fish Hoek. De-  
284 partment of Oceanography UCT, Internal report.
- 285 Dufois, F. and Rouault, M., 2012. Sea surface temperature in False Bay (South Africa): to-  
286 wards a better understanding of its seasonal and inter-annual variability. *Continental Shelf*  
287 *Res.* 43, 24-35.
- 288 Engelbrecht, F., Landman, W.A., Engelbrecht, C., Landman, S., Bopape, M.M., Roux, B.,  
289 McGregor, J.L. and Thatcher, M. 2011. Multi-scale climate modelling over Southern Africa  
290 using a variable-resolution global model. *Water SA*, 37, 647-658.
- 291 Giljam R. 2002. The effect of the Cape Flats aquifer on the water quality of False Bay. MSc  
292 Thesis, Univ. Cape Town.
- 293 Griffiths, C., Robinson, T., Lange, L., Mead, A. 2010. Marine biodiversity in South Africa –  
294 state of knowledge, spatial patterns and threats. *PloS One* 5(8): e123008.
- 295 Grundlingh, M., Hunter, I., & Potgieter, E. 1989. Bottom currents at the entrance to False  
296 Bay. *Continental Shelf Research*, 9, 1029-1048.
- 297 Grundlingh, M., and Largier, J. 1991. Physical oceanography of False Bay: a Review. *Trans*  
298 *royal soc S Afr* 47, 387-400.
- 299 Hughes, P. and Brundrit, G.B. 1991. The vulnerability of the False Bay coast line to the pro-  
300 jected rise in sea level, *Trans Roy Soc S Afr* 47, 519-534.
- 301 Hurlburt, H.E. and co-authors. 2009. High resolution global and basin-scale ocean analyses  
302 and forecasts. *Oceanography* 22, 110-127.
- 303 Jacobson, M., Hermes, J., Jackson-Veitch, J., & Halo, I. 2014. The influence of a spatially  
304 varying wind field on the circulation and thermal structure of False Bay during summer: a  
305 numerical modelling study. Dept Oceanography, UCT Internal Report.
- 306 Johnson H.K., Vested, H.J., Hersbach, H., Højstrup, J. and Larsen, S.E. 1999. The coupling  
307 between wind and waves in the WAM Model. *J. Atmos. Oceanic Technol.* 16, 1780-1790.
- 308 Joubert, J.R. and vanNiekerk, J.L. 2013. South African wave energy resource data, a case  
309 study, Stellenbosch, CRSES Internal Report, Stellenbosch.
- 310 Jury, M.R. 1991. The weather of False Bay, *Trans Roy Soc S Afr* 47, 401-427
- 311 Jury, M.R. and Reason, C.J., 1989. Extreme subsidence in the Agulhas-Benguela air mass  
312 transition, *Bound Layer Meteorol*, 46, 35-51.



- 313 Jury, M.R. and Brundrit, G.B. 1992. Temporal organisation of upwelling in the southern  
314 Benguela ecosystem by resonant coastal trapped waves in the ocean and atmosphere, S. Afr.  
315 J. Marine Science, 12, 219-224.
- 316 Largier, J.L., Chapman, P., Peterson, W.T., Swart, V.P. 1992. The Western Agulhas Bank —  
317 circulation, stratification and ecology. S Afr J Marine Sci 12: 319-339.
- 318 Lloyd, P., Plaganyi, E.E., Weeks, S.J., Magno-Canto, M. and Plaganyi, G. 2012. Ocean  
319 warming alters species abundance patterns and increases species diversity in an African  
320 subtropical reef-fish community. Fish Oceanogr. 21, 78-94.
- 321 Lutjeharms, J.R.E. and Stockton, P.L. 1991. Aspects of the upwelling regime between Cape  
322 Point and Cape Agulhas, South Africa. S Afr J Marine Sci 10: 91-102.
- 323 Mather, A., Garland, G. and Stretch, D. 2009. Southern African sea levels: corrections,  
324 influences and trends. Afr. J. Marine Science, 31, 145-156.
- 325 Metzger, E.J. and co-authors. 2014. US Navy operational global ocean and Arctic ice  
326 prediction systems. Oceanography 27, 32-43.
- 327 Metzger, E.J., Helber, R.W., Hogan, P.J., Posey, P.G., Thoppil, P.G., Townsend, T.L.,  
328 Wallcraft, A.J., Smedstad, O.M., Franklin, D.S., Zamudio-Lopez, L. and Phelps, M.W. 2017.  
329 (HYCOM-NCODA) Global Ocean Forecast System 3.1 validation testing, NRL/MR/7320-  
330 17-9722, <[www.7320.nrlssc.navy.mil/pubs/2017/metzger-2017.pdf](http://www.7320.nrlssc.navy.mil/pubs/2017/metzger-2017.pdf)>
- 331 Nelson, G., Cooper, R.M., and Cruickshank, S. 1991. Time series from a current meter array  
332 near Cape Point, Trans Roy Soc S Afr 47, 471-482.
- 333 Nicholson, S.A. 2011. The circulation and thermal structure of False Bay: a process-oriented  
334 numerical modelling and observational study, MSc Thesis. Dept. Physical Oceanography,  
335 Univ. Cape Town.
- 336 Parsons, R.P. 2000. Assessment of the impact of the Cape Flats on surrounding water bodies.  
337 S. Peninsula Muni. Report 074/SPM-1, Somerset West.
- 338 Penven, P., Brundrit, G.B., deVerdiere, C.A., Freon, P., Johnson, A.S., and Shillington, F.A.  
339 2001. A regional hydrodynamic model of upwelling in the Southern Benguela. S. African J.  
340 Science 97, 472-475.



- 341 Pfaff, M.C., and 31 coauthors. 2019. A synthesis of three decades of socio-ecological change  
342 in False Bay, South Africa: setting the scene for multidisciplinary research and management.  
343 *Elem Sci Anth*, 7: 32. doi.org/10.1525/elementa.367
- 344 Rautenbach, C. 2014. The influence of a space varying wind field on wind-wave generation  
345 in False Bay, South Africa. SAMSS conference. Stellenbosch.
- 346 Reynolds, R.W., Rayner, N.A., Smith, T.M., Stokes, D.C., and Wang, W. 2002. An improved  
347 in situ and satellite SST analysis for climate. *J Climate* 15, 1609-1625.
- 348 Rouault, M., Pohl, B. and Penven, P. 2010. Coastal oceanic climate change and variability  
349 from 1982 to 2009 around South Africa. *Afr. J. Marine Science*, 32, 237-246.
- 350 Roux, G.B. & Toms, G. 2013. Reduction of seawall overtopping at the Strand. Stellenbosch  
351 University, Internal Report.
- 352 Saha, S. and co-authors. 2014. The NCEP Climate Forecast System version 2. *J. Climate*, 27,  
353 2185-2208.
- 354 Schlegel, R.W., Oliver, E.C., Wernberg, T., Smit, A.J. 2017. Nearshore and offshore co-  
355 occurrence of marine heatwaves and cold-spells. *Prog Oceanogr.* 151, 189-205.
- 356 Schilperoort, D.E., Shillington, F., Hermes, J., and Rautenbach, C. 2013. Investigation into  
357 the capability of the Conformal-Cubic Atmospheric Model in representing the wind fields  
358 and patterns over the False Bay region in comparison to NCEP/NCAR and observational da-  
359 ta. Department of Oceanography, UCT Internal Report.
- 360 Shannon, L.V. and Field, J.G. 1985. Are fish stocks food-limited in the Southern Benguela  
361 pelagic ecosystem? *Mar Ecol Prog Ser* 22(1), 7-19. doi:10.3354/meps022007.
- 362 Skamarock, W.C., Klemp, J.B., Dudhia, J., Gill, D.O., Barker, D.M., Huang, X., Wang, W.  
363 and Powers, J.G. 2008. A description of the Advanced Research WRF v3. NCAR Tech Note,  
364 475 pp.
- 365 Tadross, M.A., Taylor, A., and Johnston, P.A. 2012. Understanding Cape Town's climate. In:  
366 Cartwright, A, Oelofse, G, Parnell, S, Ward, S. (eds) *Climate change at the city scale: im-*  
367 *pacts, mitigation and adaptation in Cape Town*, Routledge, 9-20.
- 368 Taljaard, S. 1991. The origin and distribution of dissolved nutrients in False Bay. *Royal*  
369 *Society of South Africa Transactions TRSAAC* 47(4/5).



- 370 Taljaard, S., van Ballegooyen, R. and Morant, P. 2000. False Bay Water Quality Review.  
371 CSIR Report ENV-SC 86: 2, Stellenbosch.
- 372 Theron, A., Rossouw, M., Barwell, L., Maherry, A., Diedericks, G., & de Wet, P. 2010.  
373 Quantification of risk to coastal areas and development: wave run-up and erosion. Science  
374 real and relevant conference. Pretoria: CSIR Internal Report.
- 375 Theron, A., Rossouw, M., Rautenbach, C., vonSaint Ange, U., Maherry, A., & August, M.  
376 2014. Determination of inshore wave climate along South African coast: phase 1 coastal  
377 hazard and vulnerability assessment. Stellenbosch: CSIR Internal Report.
- 378 Theron, A., Rossouw, M., Rautenbach, C., van Niekerk, L., Luck-Vogel, M., & Cilliers, L.  
379 2014. South African coastal vulnerability assessment: phase 2. Stellenbosch: CSIR internal  
380 report.
- 381 Tolman, H.L. 2002. User manual and system documentation of WAVEWATCH-III version  
382 2.22. NCEP Tech. Note, Washington, 139 pp.
- 383 vanBallegooyen, R. 1991. The dynamics relevant to the modelling of synoptic scale  
384 circulations within False Bay. Trans royal soc S Afr 47, 419-431.
- 385 Wainman, C.K., Polito, A., Nelson, G. 1987. Winds and subsurface currents in the False bay  
386 region, South Africa. S. Afr. J. Marine Science 5: 337-346.
- 387 World Ocean Atlas. 2013. Locarnini, R.A., Zweng, M.M. and co-authors: Temperature / Sa-  
388 linity, NOAA Atlas NESDIS 73 / 74, 40 / 39 pp. (observation density).
- 389



390 **Table 1**

391

ACRONYM	NAME	SOURCE
ASCAT	Advanced Scatterometer Reanalysis	Univ Hawaii APDRC
CFSr2	Coupled Forecast System v2 reanalysis	Univ Hawaii APDRC
CHIRPS	Climate Hazards InfraRed Precipitation with Station v2	UCB via IRI Clim.Library
ECMWF	European Centre for Medium-Range Weather Forecasts v5	Climate Explorer
HYCOM	Hybrid Coordinate Ocean Model v3.1 reanalysis	Univ Hawaii APDRC
IMT	Institute for Maritime Technology of South Africa	Station data on request
MADIS	Meteorological Assimilation and Data Ingest System	NCEP
MODIS	Moderate imaging Infrared Spectrometer	USGS via IRI Clim.Library
NASA	National Aeronautics and Space Administration	NASA-giovanni
NAVGEN	US Navy global environmental model v1.4	Coastwatch Erddap
NOAA	National Oceanic and Atmospheric Administration	NOAA via IRI Clim.Library
VIIRS	Visible Infrared Imaging Radiometer Suite	Coastwatch Erddap
W3	Wavewatch v3 ocean swell reanalysis	Univ Hawaii APDRC

392 HYCOM information:

393 [www.hycom.org/hycom/documentation](http://www.hycom.org/hycom/documentation)

394 Satellite information:

395 [www.wmo-sat.info/oscar/gapanalyses?mission=12](http://www.wmo-sat.info/oscar/gapanalyses?mission=12)

396 [www.wmo-sat.info/oscar/gapanalyses?mission=13](http://www.wmo-sat.info/oscar/gapanalyses?mission=13)

397 [www.wmo-sat.info/oscar/gapanalyses?variable=133](http://www.wmo-sat.info/oscar/gapanalyses?variable=133)

398 [www.wmo-sat.info/oscar/gapanalyses?variable=148](http://www.wmo-sat.info/oscar/gapanalyses?variable=148)



399 **Table 2:** Relative influence of surface weather observations in model assimilation, with grey  
 400 land mask. Stations reporting (in 2020): land-based private ○ official ●, marine-based on-  
 401 line ✓ off-line ✗. Curved line is routine aircraft wind / temp profile; sources: NASA, NO-  
 402 AA, MADIS, Wundermap.

33.85S	0.91	0.92	0.92	0.92	0.92	0.94	0.95	0.96	1.05
33.95S	0.88	0.94	0.89	0.89	0.89	0.90	0.91	0.91	1.03
34.05S	0.42	0.38	0.34	0.28	0.28	0.28	0.31	0.37	0.78
34.15S	0.40	0.34	0.31	0.24	0.24	0.24	0.28	0.31	0.77
34.25S	0.34	0.33	0.30	0.21	0.21	0.24	0.26	0.28	0.76
34.35S	0.34	0.30	0.27	0.24	0.24	0.19	0.22	0.26	0.74
34.45S	0.30	0.30	0.21	0.16	0.16	0.18	0.22	0.25	0.62
34.55S	0.15	0.16	0.15	0.16	0.16	0.16	0.18	0.22	0.50
lat / lon	18.25E	18.35E	18.45E	18.55E	18.65E	18.75E	18.85E	18.95E	19.05E

403  
 404

405 **Table 3:** Correlation of daily time series in the period December 2012 to February 2013:  
 406 HYCOM surface layer temperature T, salinity S and zonal current U<sub>c</sub> (pt 1, 3; cf. Fig 4a),  
 407 ASCAT wind U V components (pt 2) at 1-day lead and W3 swell height (pt 4). Values >  
 408 |0.27| are significant at 90% confidence (bold) with ~40 degrees of freedom.  
 409

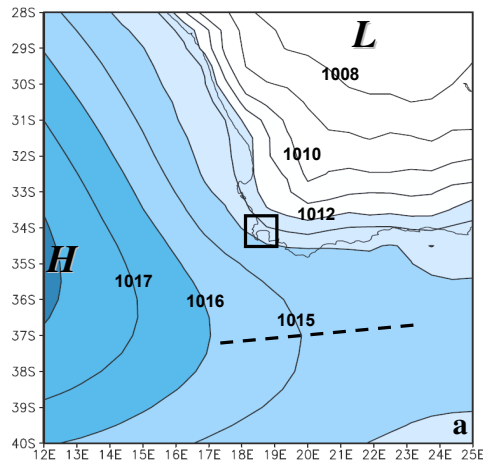
N=89	T1	T3	S1	S3	Uc1	Uc3	V-1	U-1
T3	0.02							
S1	-0.14	0.26						
S3	<b>-0.43</b>	<b>0.74</b>	<b>0.56</b>					
Uc1	0.06	0.16	-0.26	0.00				
Uc3	0.08	0.13	-0.25	-0.02	<b>0.96</b>			
V-1	-0.03	-0.05	0.26	0.06	<b>-0.68</b>	<b>-0.78</b>		
U-1	0.08	<b>0.33</b>	-0.14	0.12	<b>0.68</b>	<b>0.72</b>	<b>-0.56</b>	
swell4	<b>-0.31</b>	0.00	-0.12	0.10	-0.10	-0.11	0.10	-0.10

410  
 411

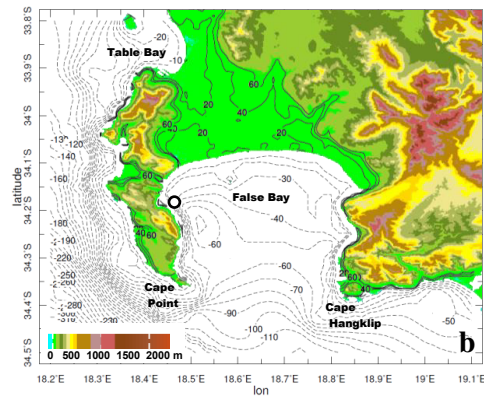


412 **FIGURES**

413



414



415

416

417

418

419

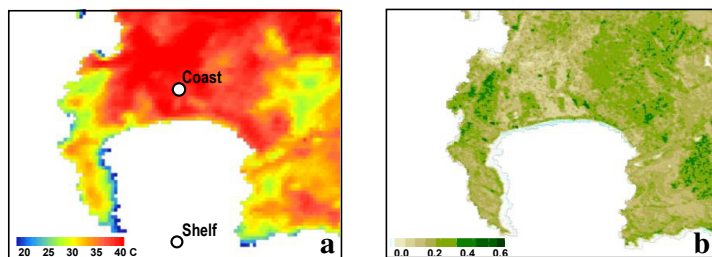
420

Fig 1 (a) Mean sea level air pressure in summer Dec 12 to Feb 13, box = False Bay area, dashed = subtropical ridge. (b) Topography (shading) and bathymetry contours; place names are labelled, dot is the IMT buoy / tide gauge / weather station off Simonstown.



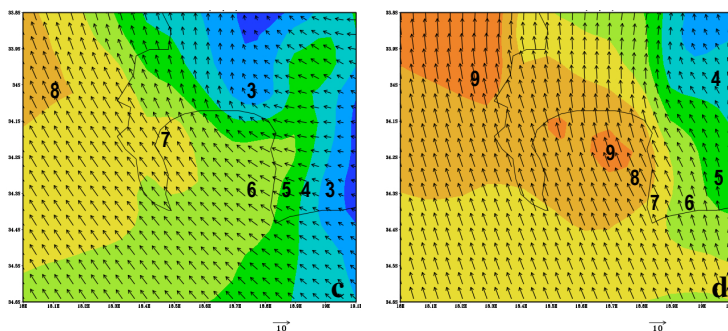


421

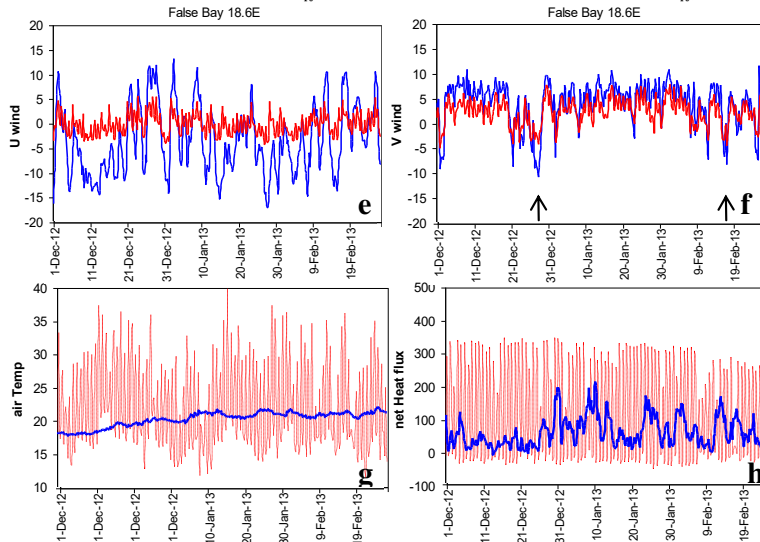


422

423



424



425

426

427

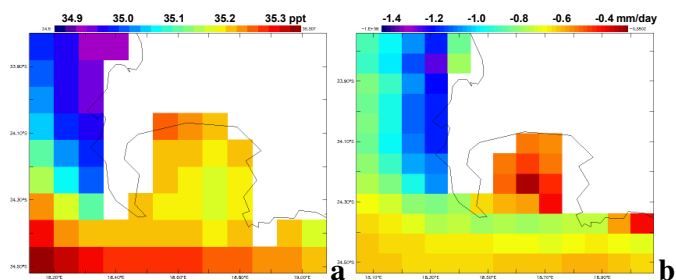
428

429

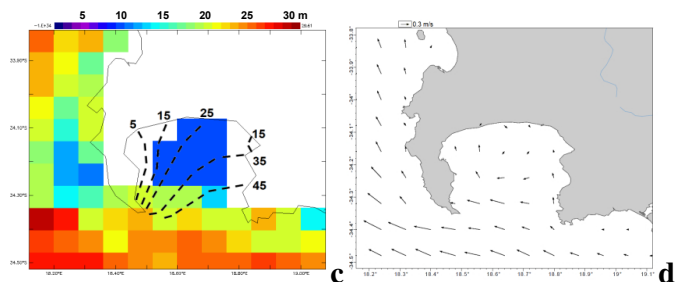
430 Fig 2 Mean conditions for summer Dec 12 – Feb 13: (a) MODIS 1 km day-time land tem-  
431 perature and (b) vegetation fraction. WRF-downscaled wind vectors and speed (shaded m/s)  
432 for Dec 12 – Feb 13: (c) 08:00 morning, (d) 14:00 afternoon. Time series Dec 12 – Feb 13 of  
433 6-hourly CFSr2 data at shelf-edge (blue) and coast (red): (e) U wind, (f) V wind, (g) air tem-  
434 perature, and (h) net heat flux. Arrows in (f) refer to coastal low/shelf wave passage noted in  
435 text.  
436



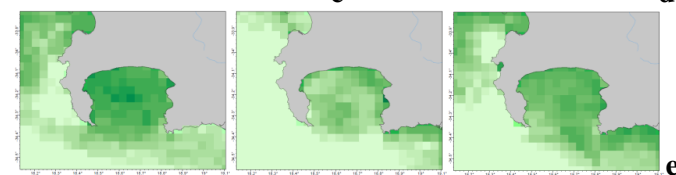
437



438

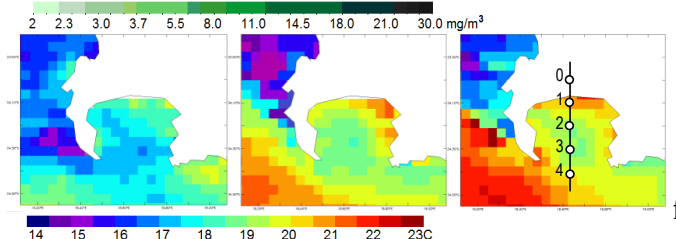


439



440

441



442

443

444

445

446

447

448

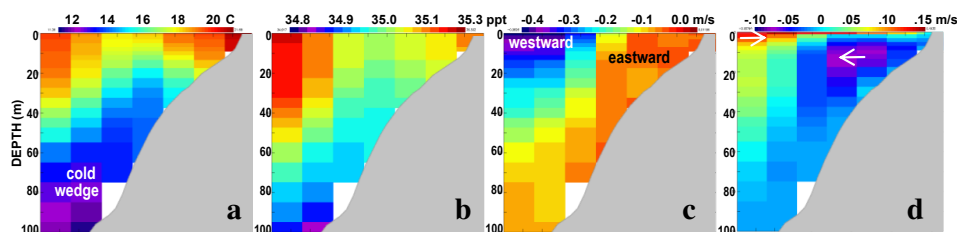
449

450

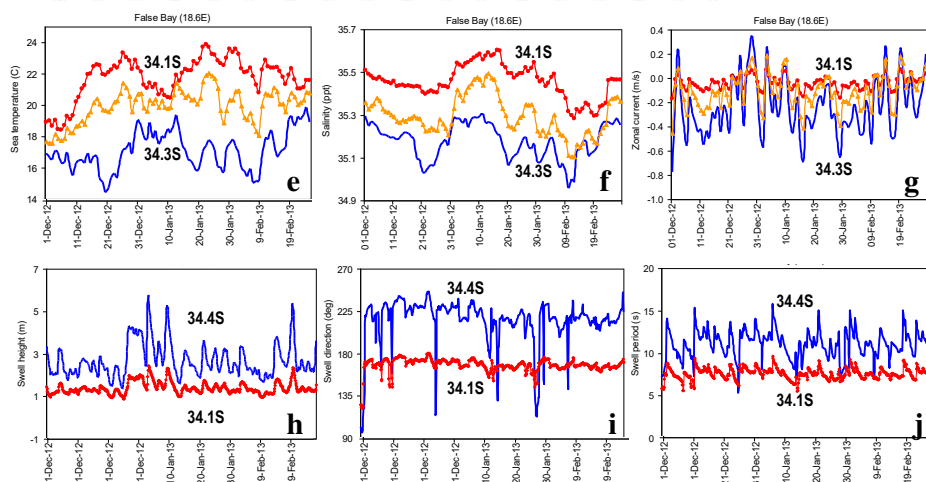
Fig 3 Mean ocean conditions for summer Dec 12 – Feb 13 from HYCOM hindcast: (a) 2 m salinity, (b) precipitation - evaporation balance, (c) mixed layer depth (m), and wave energy isolines (kW/m, after Joubert and vanNiekerc 2013) and (d) 6 m currents; with raster shading at native resolution. Sequences of Dec 12 (left) to Feb 13 monthly 4 km satellite: (e) VIIRS ocean color (chlorophyll), and (f) MODIS sea surface temperature (C). Points in (f) indicate virtual stations for time series, Table 2 statistics, and the depth section in Fig 4a-d.



451



452



453

455

456

457

458

459

460

461

462

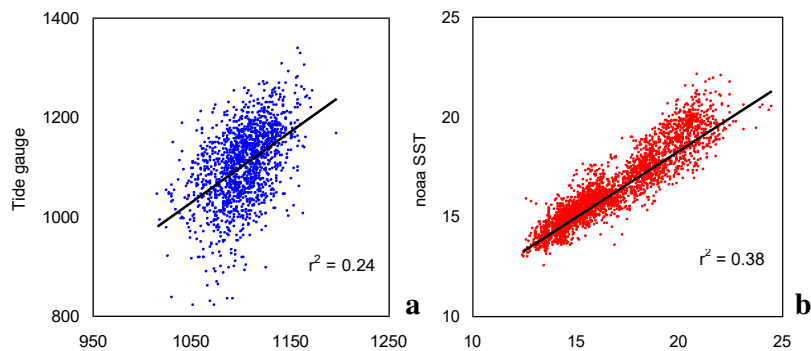
463

Fig 4 HYCOM mean summer Dec 12 – Feb 13 depth section along 18.6E: (a) temperature, (b) salinity, (c) zonal current, (d) meridional current; with shelf profile. (e,f,g) Surface layer T, S, U time series at points 1-3. Ocean wave time series Dec 12 – Feb 13 from W3 data at pts 1, 4: (h) swell height, (i) swell direction, (j) swell period. Shelf-edge is plotted –blue, mid-bay –orange, coastal –red.

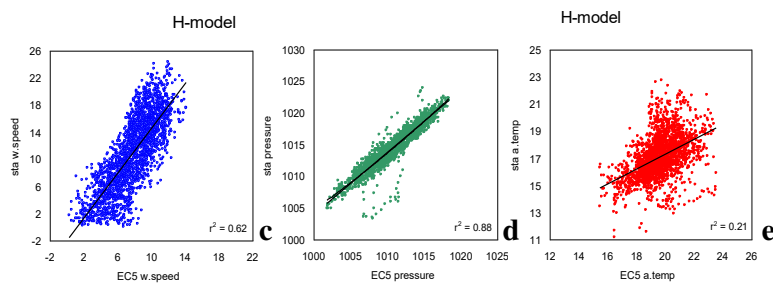


464 **Appendix**

465



466



467

468

469

470

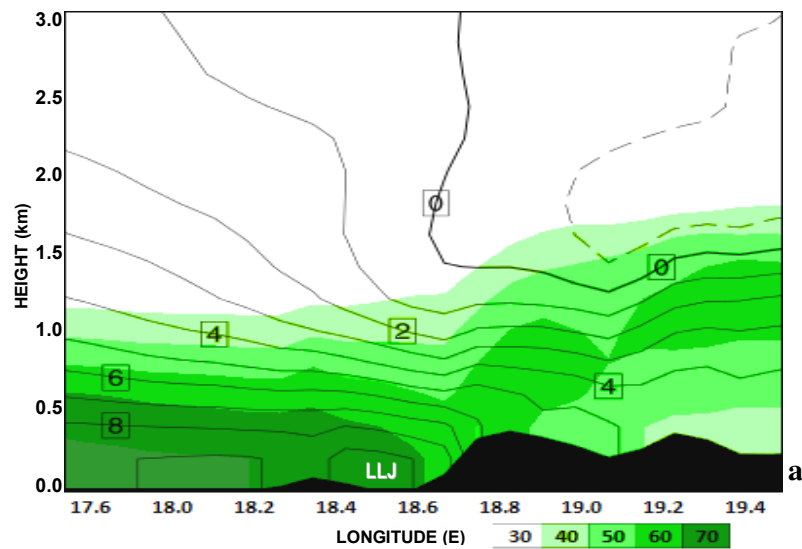
471

472

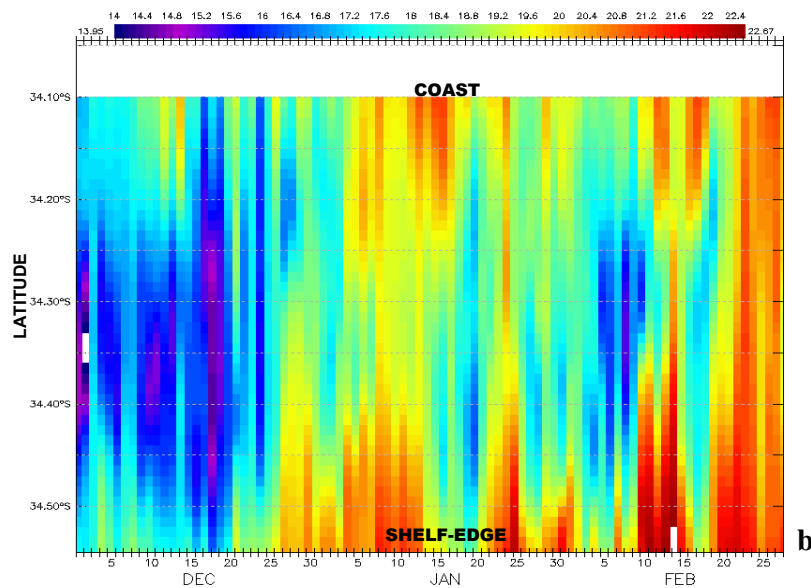
A-1 Comparison of daily HYCOM model at nearest grid-point and: (a) sea surface height from tide gauge off Simonstown in western False Bay (cf. Fig 1b) and (b) sea surface temperature from NOAA satellite; 2008-2015. Lower: Comparison of hourly ECMWF v5 reanalysis at nearest grid-point and weather station observation off Simonstown in western False Bay, 1 Dec 12 – 28 Feb 13: c) wind speed, d) pressure, and e) air temperature.



473  
474



475  
476



477 A-2 a) down-scaled WRF meridional wind isotachs and humidity % (shaded) in Dec 12 – Feb  
478 13, plotted in vertical section on 34.1S, identifying the shallowness of equatorward flow, cor-  
479 responding with Fig 2c,d. b) Hovmöller plot of daily 1 km SST on 18.6E, assimilated by  
480 GHR L4 satellite product, along the same line as Fig 4.  
481